Communication

Design of a Selective Metal Ion Switch for Self-Assembly of Peptide-Based Fibrils

Steven N. Dublin, and Vincent P. Conticello

J. Am. Chem. Soc., **2008**, 130 (1), 49-51 • DOI: 10.1021/ja0775016

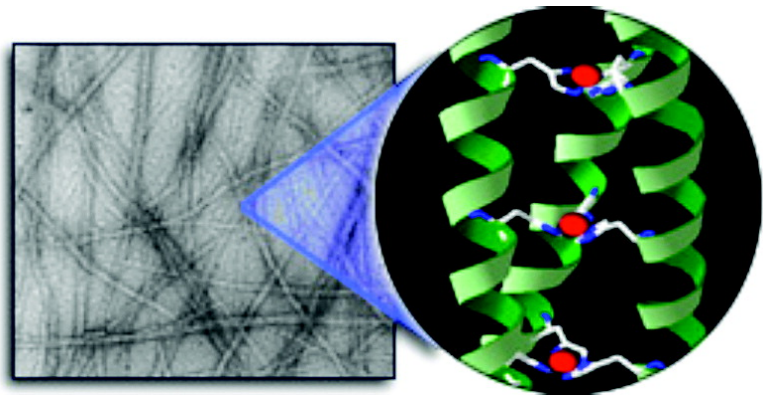

J|A|C|S
COMMUNICATIONS

Published on Web 12/08/2007

Design of a Selective Metal Ion Switch for Self-Assembly of Peptide-Based Fibrils

Steven N. Dublin and Vincent P. Conticello*

Department of Chemistry, Emory University, 1515 Dickey Drive, Atlanta, Georgia 30322

Received September 28, 2007; E-mail: vcontic@emory.edu

Nearly one-fourth of all structurally characterized proteins contain prominent metal ion binding sites.[1] These metal ions frequently play critical functional roles that include stabilization of protein structure, induction of conformational transitions, and facilitation of electron transfer, small-molecule transport, and enzymatic catalysis. Numerous peptide models have been examined to define and potentially replicate the native functional roles of metal ions within defined polypeptide structural contexts.[2] One of the most striking observations to emerge from these studies is the ability of metal ions to induce conformational transitions from the unfolded to the folded state[3−6] or between different folded states[7] through interaction with the side chains of appropriately placed amino acid ligands within the polypeptide. Moreover, metal ions can influence the supramolecular assembly of disease-related protein complexes, either enhancing or inhibiting the process, depending on the stereoelectronic properties of the specific metal.[8] In this communication, we report the ability of silver(I), a non-native metal ion, to selectively drive a conformational transition that triggers the self-assembly of a de novo designed peptide into a structurally defined nanoscale material through complexation to an engineered binding site.

Previously, we described the design and synthesis of a peptide, **TZ1H** (Figure 1),[9] based upon a trimeric coiled-coil structural motif, that self-assembled into long aspect ratio helical fibrils[10−15] at pH values above the pK_a of histidine residues that occupied structurally critical positions within the hydrophobic core. The amino acid sequence of **TZ1H** was based on that of the isoleucine zipper peptide GCN4-pII,[16] which, on the basis of prior structural analyses, had demonstrated a strong preference for formation of a three-stranded helical bundle. In addition, the design of the **TZ1H** sequence specified a network of potential electrostatic interactions between the charged *e*- and *g*-residues that would be fully complementary only in a staggered alignment in which the peptides self-assembled into a helical fibril with an axial stagger of two heptads, or one-third of the peptide length, between structurally adjacent helical protomers within the three-stranded rope (Figure 1).

The successful pH-triggered formation of the self-assembled helical fibrils validated the structural principles underlying the design of **TZ1H**;[9] however, we also noted that the layers of three proximal histidine residues within the suppositious fibril structure provided a potential metal ion binding site and, therefore, a mechanism for coupling a metal-ion-induced conformational transition to peptide self-assembly. The trigonal planar geometry within the hypothetical metal ion binding site, while infrequently encountered, has precedence for some electron-rich late transition metal ions. In particular, the silver(I) ion can adopt trigonal planar coordination in the presence of soft-donor nitrogen ligands, such as substituted imidazoles, pyrazoles, and pyridines,[17] with minimal deviations from the idealized geometry in sterically unconstrained systems.[18] We anticipated that peptide **TZ1H** could sterically accommodate the silver(I) ion within the trimeric binding site as larger ionic species have been observed as guests within cavities

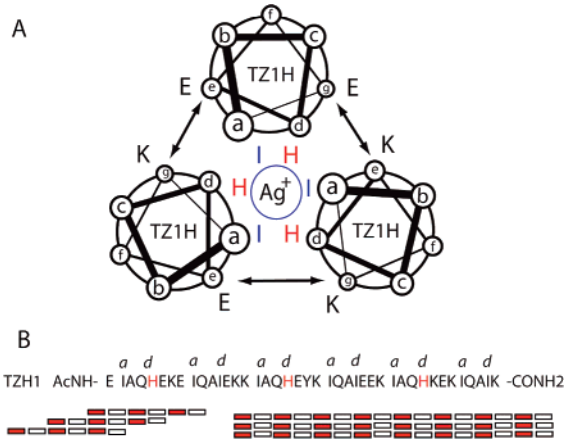

Figure 1. (A) Helical wheel diagram of a cross section of the trimeric coiled-coil depicting the suppositious silver ion binding site. (B) Amino acid sequence of **TZ1H** depicting the three core histidine residues. The proposed packing arrangement of peptides of **TZ1H** in the α-helical fibril is shown below. The staggered alignment arises from an axial displacement between adjacent protomers (red, His-containing heptads; white, non-His-containing heptads).

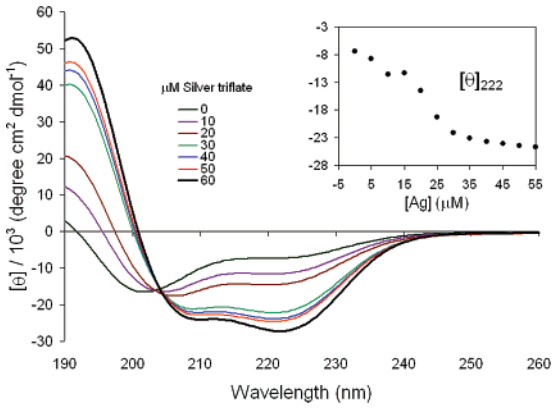

Figure 2. Dependence of the CD spectra of **TZ1H** (50 μM, 10 mM Na_2HPO_4, pH 5.6) on silver(I) ion concentration at 4 °C. Inset: Dependence of $[\theta]_{222}$ on silver(I) ion concentration.

created between similarly sized residues in trimeric coiled-coil structures.[19]

In order to test this hypothesis, circular dichroism (CD) spectropolarimetry was employed to evaluate the effect of silver(I) ion concentration on the conformation of **TZ1H** in solution at pH values below the pK_a of the core histidine residues (Figure 2). Peptide **TZ1H** (50 μM in 10 mM phosphate buffer, pH 5.6) was titrated with silver(I) triflate in a concentration range from 0 to 55 μM. In the absence of metal ions, the CD spectrum of peptide **TZ1H** displays a minimum at approximately 201 nm, which is consistent with a random coil conformation in which the charged imidazole side chains preclude formation of an α-helical conformation.[9] As

the concentration of silver(I) ion increases, a conformational transition is observed in the CD spectroscopic manifold, in which well-developed minima appear at 208 and 222 nm. These spectroscopic features, as well as the observed isodichroic point at 204 nm, are consistent with a quasi-two-state, coil-helix conformational transition as a function of silver(I) ion concentration. Thermal unfolding of the helical state of **TZ1H** was followed by CD spectropolarimetry and was fully reversible within the temperature range from 30 to 98 °C, with a T_m observed at approximately 69 °C for 70 μM peptide in the presence of equimolar silver(I) ion (cf. Supporting Information).

The nature of the conformational switch can be more easily discerned from the dependence of the mean residue ellipticity for the α-helix, $[\theta]_{222}$, on the silver(I) ion concentration (Figure 2, inset). A conformational transition is observed in which the helicity approaches a maximal value at an equimolar ratio of peptide to silver(I) ion. Further addition of silver(I) afforded no further change in helicity of **TZ1H**, which implies saturation of the metal ion binding sites of the peptide under these conditions. The specificity of the silver ion effect was investigated through selective removal of the silver(I) ion by complexation with thiosulfate anion,[20] which resulted in loss of the α-helical CD signature and concomitant formation of random coil (cf. Supporting Information). In contrast, the addition of excess EDTA to the **TZ1H**−silver ion complex had a negligible effect on the helicity of the specimen due the low formation constant of the silver(I)−EDTA complex.[21] These observations suggest that the silver ion exerts a specific effect on the conformation of peptide **TZ1H**, presumably as a result of selective binding to the histidine residues.

The role of the histidine residues in silver ion binding can be indirectly ascertained through the effect of pH on the silver-ion-induced conformational transition. CD spectropolarimetry was used to investigate the influence of pH on the metal-induced conformational change in the **TZ1H** system. Aliquots of peptide **TZ1H** (50 μM) in 10 mM phosphate buffer were prepared across a pH gradient that ranged from 4.4 to 6.0 in 0.3 pH-unit increments. After incubation at 4 °C, silver(I) triflate was added to each sample to adjust the final concentration of 25 μM silver, resulting in a 0.5 metal/peptide molar ratio. Mean residue ellipticity at 222 nm, $[\theta]_{222}$, was determined as a function of pH (cf. Supporting Information). The observed MRE values were weakly negative within the pH range from 4.0 to 5.0, indicating marginal helicity. However, a large change in $[\theta]_{222}$ was observed over the pH range from 5.2 to 5.8, which approached a limiting value at higher pH. In addition, at lower pH values, a much higher concentration of silver(I) ion was required to induce a coil-to-helix conformational transition equivalent to that observed for an equimolar silver ion/peptide ratio at pH 5.6. For example, at pH 5.3, a 4-fold molar excess of silver(I) ion was required to induce a fractional helicity value for **TZ1H** that was comparable to that observed for a 1:1 silver/peptide complex at pH 5.6. These data suggest that the silver(I) ions are in direct competition with protons for the basic lone pairs of the free imidazole nitrogen atoms of the histidine residues, and that silver ion coordination is the driving force for the conformational transition observed for **TZ1H**.

Isothermal titration calorimetry was employed to gain a quantitative determination of the binding energetics of silver(I) ion to peptide **TZ1H** under conditions that coincided with the conformational transition. Silver(I) triflate was titrated into solutions of peptide **TZ1H** (70 μM) in phosphate buffer (10 mM, pH 5.6) at 5 °C. The reaction was exothermic under these conditions, as indicated by negative values for the enthalpy of addition of the silver(I) ion (see Supporting Information). The resulting titration curves were

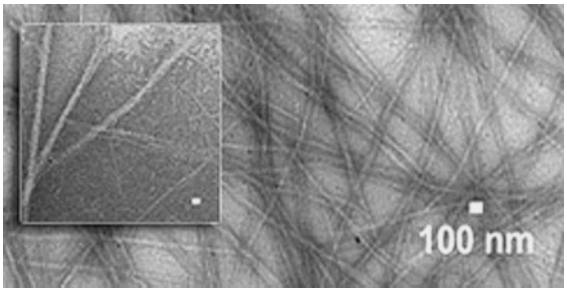

Figure 3. Unstained TEM image of long aspect ratio fibers resulting from silver(I)-ion-induced self-assembly of peptide **TZ1H**. Inset: High magnification TEM image of the small diameter fibrils that self-associate to form the larger diameter fibers (scale bar = 10 nm).

fit to a single-site model, which resulted in a binding constant (K_b) of (6.49 ± 0.523) × 10^4 M^{-1}. The value for the binding stoichiometry, *N*, was experimentally determined to be 0.91 ± 0.02, which most closely corresponded to a situation in which one silver(I) ion was bound per peptide. Thus, the experimental value of *N* correlates well with the CD data, in which an equimolar ratio of silver(I) ion to peptide was observed to have the maximal effect on the coil-to-helix transition. Theoretically, each **TZ1H** peptide can contribute one histidine residue to each of three structurally indistinguishable trigonal planar binding sites for silver ion coordination (Figure 1). Thus, within the trimeric coiled-coil structure, each histidine contributes one-third of the coordination environment for a net value of one binding site, that is, one silver(I) ion per peptide.

Conventional TEM was employed to analyze for the presence of helical fibers derived from self-assembly of **TZ1H**. Prior experimental studies of the pH-directed self-assembly of **TZ1H** indicated that fiber formation coincided with the coil-to-helix conformational transition.[9] At pH values below the pK_a of the histidine residues, negligible evidence was obtained for presence of self-assembled species, while, at higher pH values, **TZ1H** self-assembled into long aspect ratio helical fibers. Similarly, in the absence of silver(I) ion, no fibers were detected in specimens of **TZ1H** in 10 mM phosphate buffer at pH 5.6. However, TEM measurements indicated the abundant formation of long aspect ratio fibers from self-assembly of **TZ1H** under equivalent conditions in the presence of equimolar silver(I) ion (Figure 3).

The morphological features of the silver-ion-induced fibers compared well with those of the pH-induced fibers. The smallest discernible features observed in the TEM images of the silver-treated specimens corresponded to fibrils with a diameter of approximately 6.5 ± 0.2 nm (Figure 3). These morphological features were similar to those observed in the pH-triggered specimens, which were postulated as arising either from single three-stranded helical ropes or from small bundles of tightly associated ropes. However, the extent of lateral association between fibrils to form the larger diameter fibers is much less extensive for the silver-ion-induced fibrils than for the pH-induced fibrils. The dominant fiber species in the former case correspond to fibril bundles with average diameters of approximately 40 ± 1.4 nm, while the pH-triggered fibers have much larger diameters and precipitate from solution at lower concentration (ca. 100 μM **TZ1H**) than the silver-ion-induced fibers (>500 μM **TZ1H**). We postulate that the differences that are observed between the pH-triggered versus silver-induced fiber specimens arise from the different mechanisms that drive self-assembly. Individual peptides within the pH-induced fibrils have negligible net charge at near-neutral pH values, while peptides within the silver-ion-induced fibers should have a net positive charge due the presence of one silver(I) ion per **TZ1H**

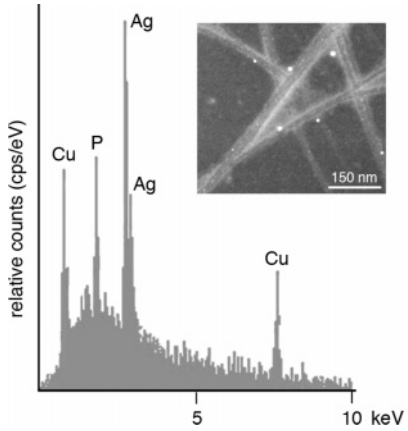

Figure 4. EDX analysis of a concentrated preparation of silver-ion-induced fibers of **TZ1H** at equimolar silver/peptide concentration. The presence of copper arises from the EM grid. Inset: Dark-field STEM image of a dispersed fibril specimen (magnification: 200K×).

peptide. The large positive charge on the latter is only partially compensated by co-localization of counterions such that Coulombic repulsion limits the extent of lateral association in comparison to the pH-induced fibers.

Direct evidence for the presence of the silver ion within the fibers was sought by employing electron microscopy methodologies. Energy-dispersive X-ray (EDX) analysis of a concentrated fiber specimen indicated the presence of elemental silver (Figure 4). The strong signature for silver can be compared to the signal for phosphorus that originates from residual phosphate from the buffer. The latter is typically present at much higher concentration (10 mM sodium phosphate versus 100−200 μM silver(I) triflate) in the initial specimen prior to isolation of the fibrils. Further confirmation for the presence of silver was obtained from elemental analysis of isolated peptide specimens, in which the silver/peptide ratio was experimentally determined to 0.90 ± 0.02, fully supporting the binding model for the silver ion depicted in Figure 1.[22] Dark-field STEM of dispersed preparations of the silver-ion-induced **TZ1H** fibers indicated electron-dense regions versus the electron-lucent carbon film background (Figure 4, inset). These results suggested the presence of a high atomic number (Z) element that co-localized with the fibril bundles, as would be expected for silver ion coordination as depicted in Figure 1.

We conclude from these studies that an appropriately chosen metal ion can drive the self-assembly of a de novo designed peptide to form a structurally defined nanoscale material. This process involves selective recognition and binding of the metal ion at a complementary site within the peptide sequence, which induces a conformational transition that results in a specific mode of self-association. Thus far, we have not addressed the issue of selectivity in metal ion binding. Although we have demonstrated that silver(I) ion can effectively induce a conformational transition and subsequent self-assembly of peptide **TZ1H**, we anticipated that other metal ions could act similarly. However, CD titration experiments indicated that neither the isoelectronic (d^{10}) zinc(II) ion, the (d^9) copper(II) ion, nor the (d^8) nickel(II) ion could effectively induce a comparable conformational transition within **TZ1H** even in the presence of excess metal ion (cf. Supporting Information). Since zinc(II), copper(II), and nickel(II) prefer alternative coordination geometries, these metal ions may not be accommodated easily within the trigonal sites of **TZ1H**. As the metal ion binding sites reside in internal cavities of the peptide assemblies, rather than at more flexible, surface-exposed sites, steric constraints are placed on the coordination geometry that, in combination with the identity and conformation of the amino acid ligands, may provide a mechanism for introducing selectivity in metal ion recognition.[3−7] Thus, the rational design of selective metal ion binding sites within de novo designed peptides represents a promising approach to the controlled fabrication of nanoscale, self-assembled materials that exploits the latent structural specificity encoded within these sequence-defined macromolecules.

Acknowledgment. V.P.C. acknowledges support from NSF (CHE-0414434) and DOE (ER-15377) grants. The authors thank Dr. Cora MacBeth for helpful discussions.

Supporting Information Available: Experimental methods and additional analyses. This material is available free of charge via the Internet at http://pubs.acs.org.

References

(1) Shi, W.; Zhan, C.; Ignatov, A.; Manjasetty, B. A.; Marinkovic, N.; Sullivan, M.; Huang, R.; Chance, M. R. *Structure* **2005**, *13*, 1473−86.
(2) (a) Lu, Y. *Inorg. Chem.* **2006**, *45*, 9930−40. (b) Hong, J.; Kharenko, O. A.; Ogawa, M. Y. *Inorg. Chem.* **2006**, *45*, 9974−84. (c) Ghosh, D.; Pecoraro, V. L. *Curr. Opin. Chem. Biol.* **2005**, *9*, 97−103. (d) Baltzer, L.; Nilsson, J. *Curr. Opin. Biotechnol.* **2001**, *12*, 355−60. (e) Benson, D. E.; Wisz, M. S.; Hellinga, H. W. *Proc. Natl. Acad. Sci. U.S.A.* **2000**, *97*, 6292−7. (f) DeGrado, W. F.; Summa, C. M.; Pavone, V.; Nastri, F.; Lombardi, A. *Annu. Rev. Biochem.* **1999**, *68*, 779−819.
(3) Petros, A. K.; Reddi, A. R.; Kennedy, M. L.; Hyslop, A. G.; Gibney, B. R. *Inorg. Chem.* **2006**, *45*, 9941−58.
(4) Kharenko, O. A.; Ogawa, M. Y. *J. Inorg. Biochem.* **2004**, *98*, 1971−4.
(5) (a) Farrer, B. T.; Pecoraro, V. L. *Proc. Natl. Acad. Sci. U.S.A.* **2003**, *100*, 3760−5. (b) Matzapetakis, M.; Farrer, B. T.; Weng, T. C.; Hemmingsen, L.; Penner-Hahn, J. E.; Pecoraro, V. L. *J. Am. Chem. Soc.* **2002**, *124*, 8042−54.
(6) (a) Tanaka, T.; Mizuno, T.; Fukui, S.; Hiroaki, H.; Oku, J.; Kanaori, K.; Tajima, K.; Shirakawa, M. *J. Am. Chem. Soc.* **2004**, *126*, 14023−8. (b) Kiyokawa, T.; Kanaori, K.; Tajima, K.; Koike, M.; Mizuno, T.; Oku, J. I.; Tanaka, T. *J. Pept. Res.* **2004**, *63*, 347−53. (c) Li, X.; Suzuki, K.; Kanaori, K.; Tajima, K.; Kashiwada, A.; Hiroaki, H.; Kohda. D.; Tanaka, T. *Protein Sci.* **2000**, *9*, 1327−33.
(7) (a) Ambroggio, X. I.; Kuhlman, B. *J. Am. Chem. Soc.* **2006**, *128*, 1154−61. (b) Cerasoli, E.; Sharpe, B. K.; Woolfson, D. N. *J. Am. Chem. Soc.* **2005**, *127*, 15008−9. (c) Pagel, K.; Vagt, T.; Kohajda, T.; Koksch, B. *Org. Biomol. Chem.* **2005**, *3*, 2500−2.
(8) (a) Dong, J.; Canfield, J. M.; Mehta, A. K.; Shokes, J. E.; Tian, B.; Childers, W. S.; Simmons, J. A.; Mao, Z.; Scott, R. A.; Warncke, K.; Lynn, D. G. *Proc. Natl. Acad. Sci. U.S.A.* **2007**, *104*, 13313−8. (b) Dong, J.; Shokes, J. E.; Scott R. A.; Lynn, D. G. *J. Am. Chem. Soc.* **2006**, *128*, 3540−2.
(9) Zimenkov, Y.; Dublin, S. N.; Ni, R.; Tu, R. S.; Breedveld, V.; Apkarian, R. P.; Conticello, V. P. *J. Am. Chem. Soc.* **2006**, *128*, 6770−1.
(10) Harbury, P. B.; Kim, P. S.; Alber, T. *Nature* **1994**, *371*, 80−3.
(11) (a) Pandya, M. J.; Spooner, G. M.; Sunde, M.; Thorpe, J. R.; Rodger, A.; Woolfson, D. N. *Biochemistry* **2000**, *39*, 8728−34. (b) Ryadnov, M. G.; Woolfson, D. N. *Nat. Mater.* **2003**, *2*, 329−32. (c) Ryadnov, M. G.; Woolfson, D. N. *Angew. Chem., Int. Ed.* **2003**, *42*, 3021−3.
(12) Ogihara, N. L.; Ghirlanda, G.; Bryson, J. W.; Gingery, M.; DeGrado, W. F.; Eisenberg, D. *Proc. Natl. Acad. Sci. U.S.A.* **2001**, *98*, 1404−9.
(13) Potekhin, S. A.; Melnik, T. N.; Popov, V.; Lanina, N. F.; Vazina, A. A.; Rigler, P.; Verdini, A. S.; Corradin, G.; Kajava, A. V. *Chem. Biol.* **2001**, *8*, 1025−32.
(14) Zimenkov, Y.; Conticello, V. P.; Guo, L.; Thiyagarajan, P. *Tetrahedron* **2004**, *60*, 7237−46.
(15) Wagner, D. E.; Phillips, C. L.; Ali, W. M.; Nybakken, G. E.; Crawford, E. D.; Schwab, A. D.; Smith, W. F.; Fairman, R. *Proc. Natl. Acad. Sci. U.S.A.* **2005**, *102*, 12656−61.
(16) Zhou, M.; Bentley, D.; Ghosh, I. *J. Am. Chem. Soc.* **2004**, *126*, 734−5.
(17) Cambridge Structural Database (version 5.27, November, 2005): Allen, F. H. *Acta Crystallogr.* **2002**, *B58*, 380−8.
(18) Hoskins, B. F.; Robson, R.; Slizys, D. A. *J. Am. Chem. Soc.* **1997**, *119*, 2952−3.
(19) Eckert, D. M.; Malashkevich, V. N.; Kim, P. S. *J. Mol. Biol.* **1998**, *284*, 859−65.
(20) Pouradier, J.; Rigola, J. *Comptes Rendus* **1972**, *275*, 515−8.
(21) Saran, L.; Cavalheiro, E.; Neves, E. A. *Talanta* **1995**, *42*, 2027−32.
(22) The silver/peptide ratio was the average of three independent determinations of silver and peptide concentration on different fiber preparations (see Supporting Information for details).

JA0775016